

# Using a moving diffraction grating to simulate the function of an acousto-optic modulator

*R. Corey, A. Schmidt, and P. Saulnier*

*Department of Physics, Gustavus Adolphus College*

*Saint Peter, MN 56082*

## ABSTRACT

We present an instructional undergraduate laboratory that introduces the student to an acousto-optic modulator (AOM) in the context of an optical heterodyning experiment. A moving diffraction grating is used to illustrate the internal functioning of an acousto-optic modulator and to make optical heterodyning experiments accessible to any undergraduate laboratory. The concepts and techniques presented can be used from the introductory through advanced level, in that, students gain direct laboratory experience with diffraction, the Doppler shift of light, construction of a Mach-Zehnder interferometer, optical path length measurements using a heterodyne technique, and sophisticated data analysis techniques.

PACS numbers: 01.50.Pa, 07.60.Ly

## I. INTRODUCTION

The heterodyning technique (an experimental arrangement in which a beat frequency is detected) is often employed in physics because of its remarkable ability to detect small changes in frequency and/or extract small signals from large noise backgrounds. Optical heterodyning is commonly employed to measure optical path length changes to high precision. The modern tool often employed in optical heterodyning experiments is the acousto-optic modulator, which utilizes the Doppler shift of light by an ultrasonic sound wave to achieve a heterodyne (beating) signal. In 1921, Brillouin first predicted that sound waves traversing a liquid, under external illumination, would give rise to an optical diffraction phenomenon similar to that produced by a diffraction grating [1]. Ten years after Brillouin's prediction, Debye and Sears [2], and Lucas and Biquard [3], independently observed this phenomenon, the so called acousto-optic effect. Currently this phenomenon has found useful application in the modulation of light intensity [4], directional control in linear scanning applications such as laser printing [5], laser cavity dumping [4], and as a means of Doppler shifting light, the application relevant to optical heterodyning experiments. Examples of modern optical heterodyning experiments include measuring vibration amplitudes and flow velocities [6] as well as the detection of small optical path length changes encountered when obtaining the surface profile of an object [7]. Imaging absorbing structures through random media using a low coherence optical heterodyning technique is also a topic of current research [8].

In this article, we use a moving diffraction grating to illustrate the function of an acousto-optic modulator in the context of an optical heterodyning experiment. A moving diffraction grating (like a moving mirror) produces an optical Doppler shift that results in a beating interference pattern which can be seen by the unaided human eye, making it an ideal teaching aid. The similarity between a moving grating and the internal functioning of many acousto-optic devices also makes it ideal for demonstrating how these devices function. A simple experimental arrangement is presented and used to measure the index of refraction of a thin glass slide.

## II. BACKGROUND

Devices utilizing the acousto-optic effect typically operate in one of two regimes, the Bragg or Raman-Nath regimes. The description of the latter is highly analogous to the moving diffraction grating employed in this experiment. The regime in to which a specific acousto-optic device falls largely depends on the spatial extent of the acoustic wave fronts in the direction transverse to propagation.

For example, the way this phenomenon is employed by acousto-optic devices operating in the Bragg regime, where the acoustic wave fronts can be approximated as infinite plane waves, may be understood with the aid of Fig. 1. Ultrasonic sound waves (typically  $> 40$  MHz) produced by a piezoelectric transducer, traverse a crystalline material with speed  $V_s$ , width  $W$ , frequency  $f_s$ , and wavelength  $\lambda_s$ , and are absorbed by an acoustic absorber. This results in a traveling sinusoidal variation in the density of the material. Changes in refractive index of the material due to this induced mechanical stress, known as photoelasticity, result in spatial perturbations in its index of refraction. For a semi-quantitative analysis, these small sinusoidal perturbations in the index of refraction may be modeled as a series of partially reflecting planes moving at the speed of sound in the medium,  $V_s$ , a distance  $\lambda_s$  apart. This is a plausible model since variations in the index of refraction result in the partial reflection of light. Constructive interference between reflected optical waves is observed when optical wave fronts reflecting from different acoustic wave fronts add in phase, that is, their path length difference is an integral multiple of the optical wavelength in the medium. Again referring to Fig. 1, constructive interference occurs when  $\overline{AO} + \overline{OB} = m\lambda/n$ , or equivalently

$$2\lambda_s \sin\theta = m\lambda/n \quad (2.1)$$

where  $\lambda_s$  is the distance between acoustic wave fronts,  $\theta$  is the incident and diffracted angle with respect to the acoustic wave fronts,  $m$  is the diffraction order, and  $\lambda/n$  is the optical wavelength in the crystalline material with average index of refraction  $n$ . This is reminiscent of Bragg diffraction of X-rays from crystalline planes [9]. In the acousto-optic effect, however, the first order maxima dominate due to the fact that light is being scattered from a sinusoidal grating, rather than a set of discrete planes. Additionally, light in the diffraction maxima undergoes a Doppler shift resulting from the fact that it has been reflected from moving sound waves. The Doppler shift,  $\Delta\nu$ , of a light wave reflected off a moving object is given, in the classical limit, by

$$\Delta\nu = 2\nu \frac{v}{c/n} \quad (2.2)$$

where  $\nu$  is the frequency of the light source in its rest frame,  $c/n$  is the speed of light in the medium, and  $v$  is the component of the reflecting object's velocity in the direction of the reflected light. From Fig. 1, the magnitude of  $v$  is given by  $\pm V_s \sin\theta$ , where the choice of sign depends on the direction of the acoustic wave front relative to the incident light beam. Combining this observation with Eqns. 2.2 and 2.1 yields a somewhat surprising result,

$$\Delta\nu = 2\nu \frac{\pm V_s \sin\theta}{c/n} = \pm f_s. \quad (2.3)$$

The magnitude of the optical Doppler shift is equal to the frequency of the sound waves produced by the ultrasonic transducer,  $f_s$ . From Eq. 2.1, it is also evident how acousto-optic devices can be utilized in linear scanning applications. By adjusting the frequency of the acoustic wave ( $\propto 1/\lambda_s$ ) a commensurate change in beam deflection ( $\sin\theta$ ) is observed. The astute reader may wonder how the Bragg condition can still be satisfied by the incoming optical wave front without adjusting the orientation of the acoustic cell. In fact, in many Bragg regime devices employed in linear scanning applications the acoustic wave front is redirected to maintain the Bragg condition [10]. Also, by adjusting the amplitude of the acoustic wave, one can control the amount of light coupled into the diffraction maxima, providing a means of amplitude modulation. Acousto-optic modulators are often employed in this fashion as high speed beam choppers.

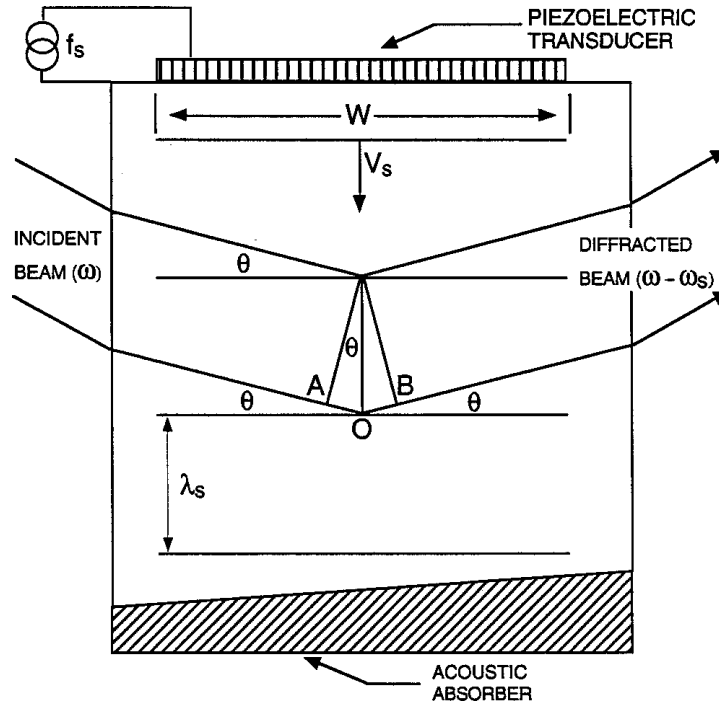


**Figure 1:** A schematic representation of an acousto-optic device operating in the Bragg regime. A piezoelectric transducer produces radio frequency sound waves that traverse the crystalline material and are absorbed by an acoustic absorber. The resulting traveling wave front spatially modulates the index of refraction of the crystal. An incoming light beam undergoes Bragg diffraction from the moving sound wave fronts. A frequency shift is observed in the diffracted light due to the Doppler effect. The magnitude of this frequency shift is equal to the frequency of the sound wave.

Several authors present an alternate, semi-quantitative model to explain the acousto-optic effect in the Bragg regime. This model examines the interaction between photons and phonons in the crystalline material [4, 11]. Still more rigorous approaches yield other important information like diffraction efficiencies and the effect of deviations from the Bragg Condition [11, 12, 13].

In the Raman-Nath [14, 15] regime the transverse extent of the acoustic wave fronts in the crystalline material is too small to be represented by infinite planes, as in the Bragg regime. In the Raman-Nath regime the sinusoidal variation of the index of refraction leads to periodic variations in the speed of light in the material, making the crystal behave like a *transmission* phase grating, yielding diffraction maxima given by the diffraction grating equation

$$m\lambda = d\sin\theta_m \quad (2.4)$$

where  $m$  is the diffraction order,  $\lambda$  is the optical wavelength in vacuum,  $\theta_m$  is the diffraction angle of the  $m^{\text{th}}$  diffraction maxima, and  $d$  is the grating spacing, in this case the acoustic wavelength in the crystal. In contrast to the Bragg Regime, the Raman-Nath regime exhibits multiple diffraction orders. Also, in this regime it is not necessary to maintain a Bragg condition, the intensity coupled to the diffraction maxima is largely independent of the angle at which light is incident on the grating. The Doppler shift,  $\Delta\nu$ , for light incident normal to and diffracting from a moving diffraction grating is given by

$$\Delta\nu = \pm \frac{V\sin\theta_m\nu}{c} \quad (2.5)$$

where  $V$  is the speed of the moving grating,  $\nu$  is the frequency of light incident on the grating, and  $c$  is the speed of light in vacuum. Substituting in for  $\sin\theta_m$ , from Eq. 2.4, and noting that  $\lambda/c = 1/\nu$ , yields

$$\Delta\nu = \pm \frac{mV}{d} \quad (2.6)$$

where again  $d$  is the grating spacing. This is the resulting Doppler shift for both a moving diffraction grating and a phase grating created by the acousto-optic effect in the Raman-Nath regime. For the case of the acousto-optic effect the grating spacing is  $\lambda_s$ , and the grating speed is  $V_s$ , reducing the equation to

$$\Delta\nu = \pm mf_s, \quad (2.7)$$

which is identical to the result obtained in the Bragg regime except for the presence of

multiple diffraction orders. We use an actual moving diffraction grating to simulate the internal functioning of an acousto-optic device operating in the Raman-Nath regime.

### III. EXPERIMENT

In a typical optical heterodyning experiment a photodetector measures a beating irradiance,  $I(t)$ , resulting from interference between the local oscillator arm and frequency shifted light from the signal arm of an interferometer. This beating irradiance is given by

$$I(t) = I_1 + I_2 + 2\sqrt{I_1 I_2} \cos(\omega_s t + \epsilon) \quad (3.1)$$

where  $I_1$ ,  $I_2$  are the irradiances of the local oscillator and signal arms respectively,  $\omega_s$  is the angular frequency difference between the two arms, and  $\epsilon$  is their relative phase [6]. Optical path length changes much smaller than a wavelength can be detected by changing the optical path length of one arm of the interferometer and measuring the resulting heterodyne phase shift relative to the undisturbed reference heterodyne signal.

The experimental configuration employed to illustrate the optical heterodyning technique is shown in Fig. 2. A low power ( $\approx 5$  mW), HeNe laser (633 nm) was used as the light source. The laser beam was expanded to allow both a reference signal and a signal with changing optical path length to pass through the upper arm of the Mach-Zehnder interferometer. Photodetector-1 (PD1) was used to measure the glass slide signal, which changes phase due to glass slide rotation, while Photodetector-2 (PD2) was used to obtain the fixed heterodyne reference signal. A diffraction grating (750 lines/mm) was mounted on a moving translation stage to simulate the functioning of an acousto-optic modulator, thereby providing the necessary Doppler shift for the heterodyne experiment. The grating was mounted such that it would translate in a direction perpendicular to the beam and grating lines. A D.C. gear-head motor, which was used to drive the ruled translation stage, was calibrated (speed versus voltage) by measuring the change in stage position for a given period of time at several voltages. The frequency shift caused by the grating moving at several speeds agreed with the theoretical prediction of Eq. 2.6. In fact, the observed frequency could be used to determine motor speed. Doppler shifts ranging from 0.1 Hz to 200 Hz, were easily observable with an oscilloscope (the lower range of these frequencies are observable with the unaided eye). It is interesting to note that this Doppler shift is from a base frequency of approximately  $5 \times 10^{14}$  Hz which represents a shift of one part in  $5 \times 10^{15}$  at the lower limit. An 80 Hz signal was used while measuring the refractive index of the glass slide. For pedagogical purposes, being able to visually observe a beating fringe pattern at low grating speeds, by

inserting a viewing card at the exit of an interferometer, has been found to be beneficial. Students can actually observe fringes moving across the pinhole in front of each detector. Actual acousto-optic modulators usually Doppler shift light by frequencies in excess of 40 MHz, yielding a beat frequency that is undetectable by the unaided human eye.

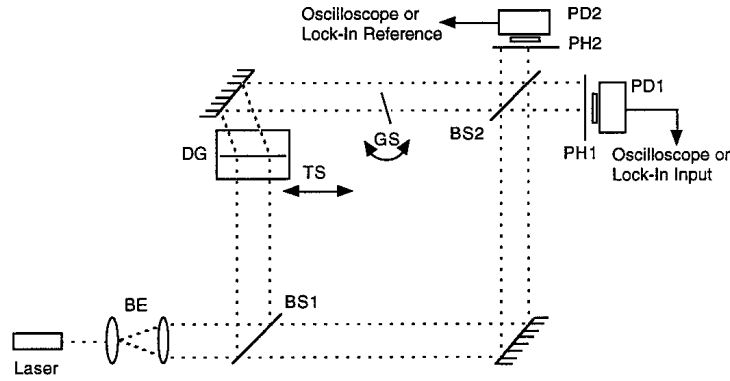


**Figure 2:** The experimental configuration used to illustrate the optical heterodyning technique and measure the index of refraction of a glass slide. A moving diffraction grating is used to simulate the internal functioning of an acousto-optic modulator and provide the required phase shift. A HeNe laser (633 nm) is used along with other major components; BE, beam expander; BS1 and BS2, beam splitters; TS, translation stage; DG, diffraction grating; GS, thin glass slide; PH1 and PH2, 800  $\mu\text{m}$  pinholes; PD1 and PD2 photodetectors. PD1 is used to obtain the phase shifted glass slide signal while PD2 measures the fixed reference signal.

A thin glass slide of thickness 0.15 mm was mounted on a graduated rotation stage such that the reference part of the beam was allowed to pass beyond its far edge, as indicated in Fig. 2. The specular reflection from the glass slide also provides an excellent means of measuring angular displacement if a graduated rotation stage is not available. This slide was rotated in discrete steps and the resulting optical path length change was measured as a phase shift (relative to the reference signal) on an oscilloscope. The slide's initial angle with respect to the incident beam was non-zero, allowing the specularly reflected beam to clear the optical arrangement, thus enabling precise angular measurements to be made. Thor Labs silicon photo-diode detectors [16] were used and are ideal for student laboratories due to their internal battery power supply, low cost, rugged housing, and high damage threshold. An 800  $\mu\text{m}$  pinhole was placed in front of each detector to allow detection of a fraction of a fringe in the beating pattern. A simple homemade pinhole will also suffice. Care was taken in the interferometer alignment to obtain fringe spacing significantly larger than the pinholes. The reference and glass slide signal were viewed on a digital oscilloscope to measure the relative phase difference

between the two signals as the glass slide rotates. For large glass slide rotations this required accumulating a total phase shift that was much greater than  $2\pi$ , corresponding to a several fringe phase shift. Relative phase changes were easily measured to within  $\pi/9$  radians, corresponding to  $1/18$  of a fringe or a change in optical path length of 35 nm. A lock-in amplifier could also easily be employed to accurately measure small phase changes. A theoretical model, derived in the next section, for the change in optical path length due to the rotation of the glass slide, was fit to the data with the slide's index of refraction as the sole fitting parameter.

#### IV. ANALYSIS AND RESULTS

In order to determine the index of refraction of the glass slide, it is necessary to measure the change in optical path length due to a rotation of the slide. Figure 3 illustrates the path taken by an incident ray passing through a glass slide when the slide's outward normal is at an angle of  $\theta_1$  with respect to the incident ray. The ray travels an optical path length,  $\Lambda_2$ , inside the glass slide given by

$$\Lambda_2 = n_2 \frac{T}{\cos\theta_2} \quad (4.1)$$

where  $n_2$  is the index of refraction of the glass slide,  $T$  is its thickness, and  $\theta_2$  is the refracted angle. In the absence of the glass slide the incident ray would travel a shorter optical path length,  $\Lambda_1$ , in traversing the same horizontal distance.

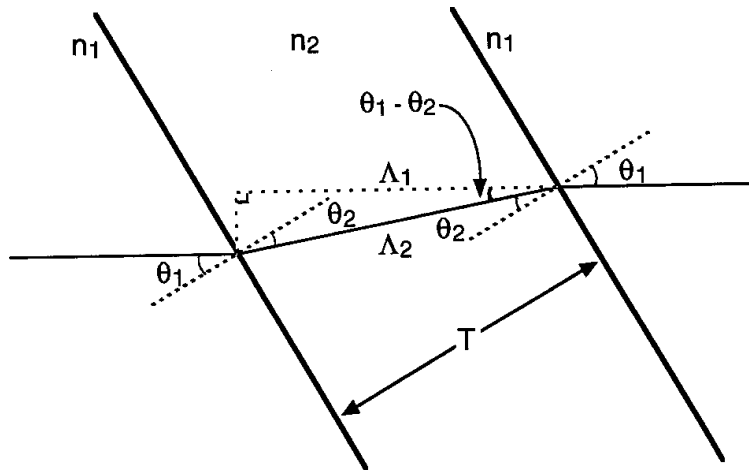


**Figure 3:** Diagram used to determine the change in optical path length of a light ray passing through a glass slide of thickness  $T$  as the slide is rotated. Light is incident on the glass slide at an angle  $\theta_1$  and is refracted to an angle  $\theta_2 < \theta_1$ . In the glass slide the light travels an optical path length  $\Lambda_2$ , whereas in the absence of a glass slide the light would travel a shorter optical path length  $\Lambda_1$  in traversing the same horizontal distance. The change in optical path length between the left and right side of the diagram for

different incident angles  $\theta_1$  is given by the change in the difference between  $\Lambda_2$  and  $\Lambda_1$ ,  $\Delta(\Lambda_2 - \Lambda_1)$  as indicated in Eq. 4.4.

This is given by

$$\Lambda_1 = \cos(\theta_1 - \theta_2) \frac{T}{\cos\theta_2} \quad (4.2)$$

where  $n_1$  is taken to be one. The increase in optical path length between the left and right side of the diagram due to the presence of the slide is given by

$$\Lambda_{slide} = \Lambda_2 - \Lambda_1 = \frac{T}{\cos\theta_2} \{n_2 - \cos(\theta_1 - \theta_2)\} \quad (4.3)$$

Thus, in rotating the glass slide from an original angle  $\theta_1$ , to a new angle  $\theta'_1$ , the net optical path length change due to the rotation is given by

$$\Delta\Lambda_{slide} = \frac{T}{\cos\theta'_2} \{n_2 - \cos(\theta'_1 - \theta'_2)\} - \frac{T}{\cos\theta_2} \{n_2 - \cos(\theta_1 - \theta_2)\} \quad (4.4)$$

where  $\theta_2, \theta'_2$  are determined from  $\theta_1, \theta'_1, n_2$ , and Snell's law. The resulting net phase change in radians is

$$\Delta\phi_{net} = \frac{2\pi}{\lambda} \Delta\Lambda_{slide}(\theta_1, \theta'_1, T, n_2) \quad (4.5)$$

where  $\lambda$  is the optical wavelength in vacuum. Measurements of this phase change as the slide is rotated, as well as a measurement of the thickness of the glass slide, yield the index of refraction of the glass slide. This was done by least-square-fitting the single parameter,  $n_2$ , in Eq. 4.5 to these measurements. The resulting fit is shown in Fig. 4 along with an inset showing two signals (reference and glass slide) as displayed on an oscilloscope, with the relative phase shift indicated. The glass slide was determined to have an index of refraction of  $1.43 \pm 0.03$ . This was verified by measuring Brewster's angle for the glass slide.

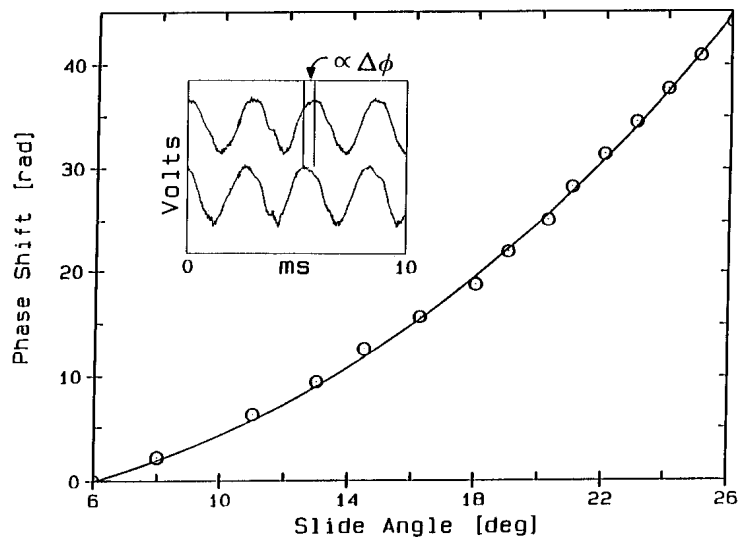


**Figure 4:** Relative phase shift between light traversing the glass slide and the undisturbed reference signal versus angle of rotation of the slide. The data was fit to a theoretical model (Eq. 4.5) with the index of refraction of the glass slide as the sole fitting parameter. Inset presents reference and glass slide signals as viewed on an oscilloscope, clearly showing a phase shift.

#### IV. CONCLUSIONS

Acoustic-optic modulators are important experimental devices in modern optics. A moving diffraction grating can be used to illustrate the internal functioning of an acousto-optic modulator and make optical heterodyning experiments accessible to undergraduate laboratories. The use of a moving diffraction grating as the Doppler shifting component allows direct observation of the beating interference pattern in an optical heterodyning experiment, greatly aiding student comprehension. We employed this technique to determine the index of refraction of a thin glass slide.

#### Acknowledgments

We are pleased to acknowledge support from a William and Flora Hewlett Foundation Award of Research Corporation and the donors of The Petroleum Research Fund, administered by the American Chemical Society, for support of this work.

## REFERENCES

- [1] L. Brillouin, "Diffusion de la lumiere et des rayons x par un corps transparent homogene influence de l'agitation thermique," *Ann. de Physique* **17**, 88-122 (1921).
- [2] P. Debye and F. W. Sears, "On the scattering of light by supersonic waves," *Proc. Nat. Acad. Sci. U.S.* **18**, 409-414 (1932).
- [3] R. Lucas and P. Biquard, "Proprietes optiques des milieux solides et liquides soumis aux vibrations elastiques ultra sonores," *J. Phys. Radium* **3**, 464-477 (1932).
- [4] F. Pedrotti and L. Pedrotti, *Introduction to Optics* (Prentice Hall, Englewood Cliffs, NJ, 1993), 2nd ed., pp. 556-559.
- [5] E. Hecht, *Lasers*, (IEEE Press, New York, NY, 1992) pp. 356-357.
- [6] P. Hariharan, *Basics of Interferometry* (Harcourt Brace Jovanovich, Boston, MA, 1992) pp. 129-131, 189.
- [7] R. Peterson, "Interferometric measurements of the surface profile of moving samples," *Appl. Opt.* **23**, 1464-1466 (1985).
- [8] A. Schmidt, R. Corey, and P. Saulnier, "Imaging through random media by use of low coherence optical heterodyning," *Opt. Lett.* **20**, 404-406 (1995).
- [9] N. Ashcroft and N. Mermin, *Solid State Physics* (Holt, Rinehart, and Winston, Philadelphia, PA, 1976) pp. 96.
- [10] L. Bademian, *Acousto-Optical Deflectors* (Isomet Corporation, Springfield, VA, 1993).
- [11] A. Yariv, *Optical Electronics* (Holt, Rinehart and Winston, New York, NY, 1985), 3rd ed., pp. 390-397.
- [12] M. Born and E. Wolf, *Principles of Optics* (Pergamon Press, New York, NY, 1970), 4th ed., pp. 593-610.
- [13] W. Klein and B. Cook, "Unified approach to ultrasonic light diffraction," *IEEE Transactions on Sonics and Ultrasonics* **14**, 123-134 (1967).
- [14] C. Raman and N. Nath, "The diffraction of light by high frequency sound waves: Part II," *Proc. Indian Acad. Sci.* **2**, 413-420 (1935).
- [15] D. Pierce and R. Byer, "Experiments on the interaction of light and sound for the advanced laboratory," *Am. J. Phys.* **41**, 314-324 (1973).
- [16] Silicon PIN photo-diode detector, item #DET1-SI, Thor Labs Inc., Newton, NJ (201) 579-7227.